NeuroImage: Clinical 35 (2022) 103077

Contents lists available at ScienceDirect

NeuroImage: Clinical

journal homepage: www.elsevier.com/locate/ynicl

Causal structure discovery identifies risk factors and early brain markers related to evolution of white matter hyperintensities

Xinpeng Shen [a,b], Sheelakumari Raghavan [b], Scott A. Przybelski [c], Timothy G. Lesnick [c], Sisi Ma [a], Robert I. Reid [e], Jonathan Graff-Radford [d], Michelle M. Mielke [c,d], David S. Knopman [d], Ronald C. Petersen [d], Clifford R. Jack Jr. [b], György J. Simon [a], Prashanthi Vemuri [b,*]

[a] Institute for Health Informatics, University of Minnesota, Minneapolis, MN, USA
[b] Departments of Radiology, Mayo Clinic, Rochester, MN, USA
[c] Quantitative Health Sciences, Mayo Clinic, Rochester, MN, USA
[d] Departments of Neurology, Mayo Clinic, Rochester, MN, USA
[e] Information Technology, Mayo Clinic, Rochester, MN, USA

ARTICLE INFO

Keywords:
Diffusion MRI
White matter health
FLAIR
White matter hyperintensities
Causal discovery

ABSTRACT

Our goal was to understand the complex relationship between age, sex, midlife risk factors, and early white matter changes measured by diffusion tensor imaging (DTI) and their role in the evolution of longitudinal white matter hyperintensities (WMH). We identified 1564 participants (1396 cognitively unimpaired, 151 mild cognitive impairment and 17 dementia participants) with age ranges of 30–90 years from the population-based sample of Mayo Clinic Study of Aging. We used computational causal structure discovery and regression analyses to evaluate the predictors of WMH and DTI, and to ascertain the mediating effect of DTI on WMH. We further derived causal graphs to understand the complex interrelationships between midlife protective factors, vascular risk factors, diffusion changes, and WMH. Older age, female sex, and hypertension were associated with higher baseline and progression of WMH as well as DTI measures ($P \leq 0.003$). The effects of hypertension and sex on WMH were partially mediated by microstructural changes measured on DTI. Higher midlife physical activity was predictive of lower WMH through a direct impact on better white matter tract integrity as well as an indirect effect through reducing the risk of hypertension by lowering BMI. This study identified key risks factors, early brain changes, and pathways that may lead to the evolution of WMH.

1. Introduction

Leukoaraiosis or white matter hyperintensities (WMH) are the hyperintense patches on T2-weighted or fluid attenuated inversion recovery (FLAIR) images. WMH are important because they are a common manifestation of cerebrovascular disease (CVD) and have a significant impact on motor and cognitive function (Whitman et al., 2001; Cees De Groot et al., 2000). They are also a predictor of increased risk of stroke and dementia (Debette and Markus, 2010). Older age and hypertension are the two well known risk factors associated with the development of WMH (Scharf et al., 2019; Habes et al., 2016; Gottesman et al., 2010; Godin et al., 2011). Recent studies show that females have higher WMH load suggesting that sex differences play a role in the evolution of WMH (Scharf et al., 2019; Fatemi et al., 2018). Even with vast literature on risk factors of WMH, a clear mechanistic understanding of the factors related to the evolution of WMH is still lacking.

Emerging evidence shows significant microstructural changes on diffusion tensor imaging (DTI) even before the appearance of WMH (Maillard et al., 2013; Maniega et al., 2015). Given the heterogeneity in the formation of WMH, our first hypothesis was that measuring early diffusion changes will aid in predicting future formation of WMH beyond the classical risk factor - hypertension. Further, evaluating midlife risk factors in the context of early diffusion changes are likely to lead to a better understanding of the mechanisms. Therefore, our second hypothesis was that midlife risk factors have an impact on WMH through early diffusion changes and measuring these early diffusion changes will allow us to identify the pathways for prevention of WMH.

Given these gaps in knowledge, our goal was to investigate the complex relationships between age, sex, midlife risk/protective factors, diffusion changes, and WMH. We evaluated this question using a large

* Corresponding author at: Mayo Clinic and Foundation, 200 First Street SW, Rochester, MN 55905, USA.
E-mail address: vemuri.prashanthi@mayo.edu (P. Vemuri).

https://doi.org/10.1016/j.nicl.2022.103077
Received 17 February 2022; Received in revised form 25 April 2022; Accepted 3 June 2022
Available online 7 June 2022

dataset (n = 1564) of longitudinal multi-modal imaging data (WMH via FLAIR MRI and fractional anisotropy or FA from DTI MRI), clinical information (related to hypertension, dyslipidemia, and diabetes), and midlife risk factors (physical activity, cognitive activity, and smoking) from the population-based sample of Mayo Clinic Study of Aging (MCSA). In addition to traditional statistical regression models, we leveraged causal structure discovery (CSD) models to study the interactions and pathways that lead to worsening WMH. The CSD methods have many strengths. As compared to traditional regression models for a specific outcome, they can model the complex (direct and indirect) relationships among all variables at the same time. Given a set of assumptions (Pearl, 2009), such as no unobserved confounders, the Causal Faithfulness condition, and the Causal Markov condition, the relationships in the causal graph admit a 'causal' interpretation. As compared to traditional structural equation modeling and path analysis, the CSD methods are data driven and can incorporate existing knowledge regarding the domain of interest (Pearl, 2009). These discovered relationships help investigate causal interpretations whereby manipulating one variable can alter other variables. These models stand in contrast to models that investigate associative relationships and have demonstrated great success in many domains such as causal relationships in anxiety disorder, image recognition, or climate prediction (Li et al., 2020; Anker et al., 2019; Ebert-Uphoff and Deng, 2012).

2. Materials and methods

2.1. Selection of participants

Participants were selected from MCSA, an epidemiological sample of residents living in Olmsted County, Minnesota. Olmsted county population was enumerated in the Rochester Epidemiology Project (REP) medical records-linkage system (Rocca et al., 2012; St Sauver et al., 2012). The details of the study design were published elsewhere (Roberts et al., 2008; Petersen et al., 2010). The inclusion criteria were cognitively unimpaired elderly with an age range of 30–90 years with usable 3 T FLAIR MRI, DTI, and cardiovascular and metabolic risk factor information.

Standard protocol approvals, registrations, and patient consents: The study was approved by the Mayo Clinic and Olmsted Medical Center institutional review boards and written informed consent was obtained from all participants.

2.2. Imaging

2.2.1. Assessment of WMH on FLAIR scans

All MRI images were acquired from 3 T MRI systems (GE Healthcare). Both 3D MPRAGE and 2D FLAIR image were used to calculate WMH volume. The acquisition and analysis of the FLAIR images were described previously (Graff-Radford et al., 2019). In brief, the possible WMH voxels on FLAIR images were identified initially through clustering via connected components . We then masked the FLAIR images using white matter (WM) masks derived from 3D MPRAGE segmentation to exclude the false-positive WMH voxels. These masks were edited by a trained analysts to remove non-WMH voxels.

2.2.2. DTI

The DTI acquisition protocol used a single-shot echo-planar imaging sequence with an isotropic resolution of 2.7 mm, 5 non diffusion-weighted images, and 41b = 1000 s/mm^2 diffusion-encoding gradient directions spread over the whole sphere. The data were preprocessed by skull stripping (Reid and Schwarz, 2018), denoising (Veraart et al., 2016), correcting for head motion and eddy current distortion (Andersson et al., 2016), Gibbs ringing (Kellner et al., 2016), and then debiasing (Koay et al., 2009). Diffusion tensors were then fit using a nonlinear least squares fitting algorithm implemented in dipy, (Garyfallidis et al., 2014) and then FA maps were generated. ANTs (Advanced normalization tools symmetric normalization) (Avants et al., 2011) was used to nonlinearly register each participant's FA image to the in-house- version of John's Hopkins University "Eve" WM atlas (Oishi et al., 2009), and then regional FA measures were computed. FA measures were computed for 12 WM tracts including genu of the corpus callosum, splenium of the corpus callosum, body of the corpus callosum, parahippocampal cingulum, cingulum, inferior temporal WM, superior longitudinal fasciculus, corticospinal tract, anterior limb of the internal capsule, posterior limb of the internal capsule, inferior fronto-occipital fasciculus, and uncinate fasciculus.

Quality assessment was performed by the visual inspection of each participant's DTI image acquisition (both raw images and DTI based FA/MD images) and registration of the JHU atlas to the images. In those who had potentially usable data, we found that a small percentage (0.28%) of corresponding DTI scans failed quality control based on visual inspection of the DTI image acquisition and processing, and those scans were not used. Separately from QC, the FA and MD values were characterized using the median of voxel values within each JHU region of interest. The median was used to reduce the partial volume contamination from the edge voxels of each region. We also excluded the voxels with MD $> 2 \times 10^{-3}$ or $< 7 \times 10^{-5}$ mm^2/s as they were mostly cerebrospinal fluid or air, respectively. Moreover, we excluded the smallest JHU regions (cuneus WM, fusiform WM, lingual WM, and precuneus WM, all typically < 7 diffusion voxels) as they were too small for reliable registration onto the corresponding subject structure, and liable to be dominated by edge voxels.

2.2.3. Assessment of cardiovascular and metabolic risk factors

The medical history of the participants was obtained from a combination of in person clinical visit or the REP medical record linkage system. We obtained the body mass index (BMI, kg/m^2), metabolic syndromes such as low-density lipoprotein (LDL), high density lipoprotein (HDL), triglycerides, systolic and diastolic blood pressure (SBP $\geq$ 140 mmHg and DBP $\geq$ 90 mmHg), and total cholesterol from REP. We also utilized nurse abstracted data from MCSA on the history of vascular risk factors including type 2 diabetes mellitus, hypertension, and dyslipidemia (Roberts et al., 2014). In addition, we utilized smoking status ascertained at the time of the clinical visit (never, current, and former). We estimated midlife physical and cognitive activity summary scores from questionnaires that were published previously (Vemuri et al., 2012) which summarizes engagement in several physical and cognitive activities.

2.3. Statistical analyses

All statistical analyses were conducted using R (v.4.0.0) and we used R package rcausal (v.1.1.1) for causal discovery. Characteristics of the participants were summarized as mean (standard deviation) for the continuous variables, and count (%) for the categorical variables stratified by age groups. The differences between age groups were compared using ANOVA and χ^2 test for continuous and categorical variables, respectively. We computed total intracranial volume using an in-house modified SPM software implementation and used WMH as a percentage of total intracranial volume (dividing by the total intracranial volume). Dividing by total intracranial volume accounts for differences in head size and is common practice in the field (Wardlaw et al., 2017). WMH was log-transformed for normality.

Risk factors associated with baseline WMH and its progression. To analyze the risk factors of WMH and WM health at baseline, we used stepwise linear regression to select predictors from cardiometabolic, clinical, and demographics risk factors. We excluded HbA1c because of missingness. Samples with missing data elements were removed from the study. Longitudinal WMH scans were measured cross sectionally and used as the measurement for WMH progression. We showed the scatterplot of WMH and age, as well as the boxplots of WMH for (i) patients with and without hypertension and (ii) male and female patients across

the five age groups. An unpaired *t*-test was used to test the WMH differences between the presence and absence of hypertension (and male and female sex) within each age group. To quantify the effect of age, sex, and hypertension on baseline WMH, an ordinary least squares multiple regression model was constructed regressing the WMH on age, sex, and hypertension status. For the longitudinal analysis, we modeled the WMH progression using linear mixed effect models (R package lmerTest, lme4) while controlling the same set of variables as in the baseline analysis. Participants with only the baseline visit were removed from this part of the analysis.

Risk factors associated with baseline WM health measured by DTI and its progression. We conducted the same set of analyses for WM health as we did for WMH.

Mediation effect of WM health on WMH. We first showed the scatterplot of WM health and WMH. We then applied mediation analysis to study the mediation effect of WM health on WMH. The steps of the mediation analysis can be found here (VanderWeele, 2016). We fitted two regression models to log-transformed WMH while controlling for the direct causes of WMH and WM. One model included WM health, and one model did not. All variables were z-transformed, so that the standardized effect sizes can be compared across models.

Effect of midlife cardiovascular risk factors on WMH and WM health (pathway to potentially preventing progression of WMH). To study the effect of intervention on WMH, we added three midlife modifiers (midlife physical activity, midlife cognitive activity, and up-to-midlife smoking status) to the models. Statistically significant ($P < 0.05$) midlife modifiers were kept in the model. To further explore the causal relationships between WMH and its potential midlife modifiers, we applied a CSD algorithm (Spirtes et al., 2000; Glymour et al., 2019), Fast Greedy Equivalence Search (Ramsey et al., 2017) (FGES) with Fisher-z score and alpha 0.01, to generate the causal graph underlying the relationships. We ran 100 bootstrap iterations on the cohort and extracted relationships that appeared in more than half of the iterations.

3. Results

We included 1564 participants, 1396 cognitively normal, 151 with mild cognitive impairment and 17 with dementia from the population-based sample of Mayo Clinic Study of Aging (MCSA). The demographics, clinical, late-life vascular risk factors, midlife risk factors, and imaging biomarkers of the participants by decade (30–49, 50–59, 60–69, 70–79, and 80–89) are shown in Table 1. 54%, 51%, 50%, 52%, and 58% of participants were male in the age range of 30–49, 50–59, 60–69, 70–79, 80–89, respectively. There were 10%, 31%, 53%, 67%, and 82% hypertensive participants across the age groups as expected. All the late-life chronic condition measurements and midlife risk factors were significantly different between the age groups ($P < 0.007$ and$P < 0.001$ respectively). The percentage of participants diagnosed with diabetes, hypertension, and dyslipidemia increased as the baseline age increased; in the age group 80–89, there were 19%, 82%, and 86% of participants with these diagnoses, respectively. Six hundred and thirty-one (40.3%) participants had more than one scan and the rest of them only had baseline imaging data available. To make use of all the available data, we conducted analyses on both the cross-sectional and longitudinal data.

3.1. Risk factors associated with baseline WMH and its progression

The overall distribution of log-transformed WMH by age is shown in the left panel, Fig. 1A. Starting from age 50, the WMH increases linearly as age increases. The right panel (Fig. 1B and 1C) shows the difference in WMH between males and females, and between participants with and without hypertension (normotensive). Student t-tests were conducted to test the within-group differences as shown at the top of each boxplot. WMH significantly differed by sex in late-life ($P \leq 0.005$ in 60–70, 70–80, and 80–90 years of age). There were significant differences in

Table 1
Participants baseline characteristics. Mean (SD) and Count (%) for continuous and categorical variables, respectively.

	30–49, n = 59	50–59, n = 262	60–69, n = 540	70–79, n = 407	80–89, n = 296	*P* value
Demographics & APOE						
Age	40.02 (5.24)	54.64 (2.46)	64.59 (2.84)	74.51 (2.91)	83.52 (2.94)	
Male	32 (54%)	133 (51%)	272 (50%)	212 (52%)	171 (58%)	0.32
APOE e4	14 (24%)	79 (30%)	154 (29%)	124 (30%)	78 (26%)	0.661
BMI	28.31 (5.87)	29.21 (5.4)	29.49 (5.43)	28.21 (4.47)	26.98 (4.2)	<0.001
Laboratory results						
LDL	102.42 (31.32)	109.13 (30.92)	103.76 (29.77)	97.3 (29.03)	90.89 (27.32)	<0.001
HDL	55.08 (18.03)	55.64 (17.85)	55.49 (17.05)	55.76 (17.36)	55.09 (16.51)	0.991
Triglycerides	119.56 (70.17)	128.87 (65.16)	130.76 (62.01)	125.95 (59.16)	123.17 (53.95)	0.425
Total cholesterol	181.42 (40.46)	190.57 (33.87)	185.42 (35.61)	178.26 (36.32)	170.6 (33.89)	<0.001
HbA1c	5.87 (1.32)	6.04 (1.12)	5.93(1)	5.95 (0.79)	5.97 (0.76)	0.912
SBP	126.19 (15.02)	131.48 (16)	139.13 (18.45)	141.15 (18.5)	142.49 (20.13)	<0.001
DBP	78.42 (10.96)	79.16 (9.34)	78.2 (9.98)	74.14 (10.05)	71.12 (10.86)	<0.001
Current Clinical Diagnosis						
Cognitively Impaired	2(3%)	7(3%)	29(5%)	62 (15%)	68 (23%)	<0.001
Diabetes	3(5%)	31 (12%)	73 (14%)	74 (18%)	56 (19%)	0.007
Hypertension	6(10%)	82 (31%)	285 (53%)	273 (67%)	244 (82%)	<0.001
Dyslipidemia	20 (34%)	169 (65%)	424 (79%)	332 (82%)	254 (86%)	<0.001
Midlife risk factors						
Midlife physical activity	8.27 (3.55)	7.39 (3.66)	9.1 (4.43)	9.11 (4.27)	9.15 (4.66)	<0.001
Midlife cognitive activity	17.07 (6.59)	20.29 (8.27)	18.62 (9.22)	20.94 (8.61)	20.87 (9.49)	<0.001
Smoking status	21 (36%)	92 (35%)	246 (46%)	205 (50%)	119 (40%)	<0.001
MRI & DTI						
Abnormal WMH	0(0%)	0(0%)	24(4%)	65 (16%)	110 (37%)	<0.001
Baseline WMH	0.18 (0.09)	0.31 (0.22)	0.56 (0.61)	1.02 (0.79)	1.74 (1.35)	<0.001
Genu of the corpus callosum FA	0.64 (0.04)	0.63 (0.04)	0.61 (0.04)	0.59 (0.05)	0.56 (0.05)	<0.001
Splenium of the corpus callosum FA	0.69 (0.03)	0.69 (0.03)	0.69 (0.04)	0.68 (0.04)	0.66 (0.05)	<0.001
Body of corpus callosum FA	0.62 (0.03)	0.61 (0.04)	0.6 (0.04)	0.59 (0.04)	0.56 (0.05)	<0.001
Anterior limb of the internal capsule FA	0.59 (0.03)	0.59 (0.03)	0.59 (0.03)	0.57 (0.04)	0.56 (0.04)	<0.001
Scan statistics						
Scan Interval, years		1.25 (0.44)	1.31 (0.45)	1.73 (0.77)	1.78 (0.87)	
Participants with 2 Scans	0(0%)	70 (27%)	200 (37%)	129 (32%)	80 (27%)	
Participants with 3 Scans	0(0%)	11(4%)	43(8%)	62 (15%)	36 (12%)	

The final samples shown in the table are the total samples utilized. Abbreviations: APOE e4: Apolipoprotein E epsilon 4; BMI: body mass index; HDL: high density lipoprotein; LDL: low density lipoprotein; SBP: systolic blood pressure; DBP: diastolic blood pressure; HbA1c: glycated hemoglobin.

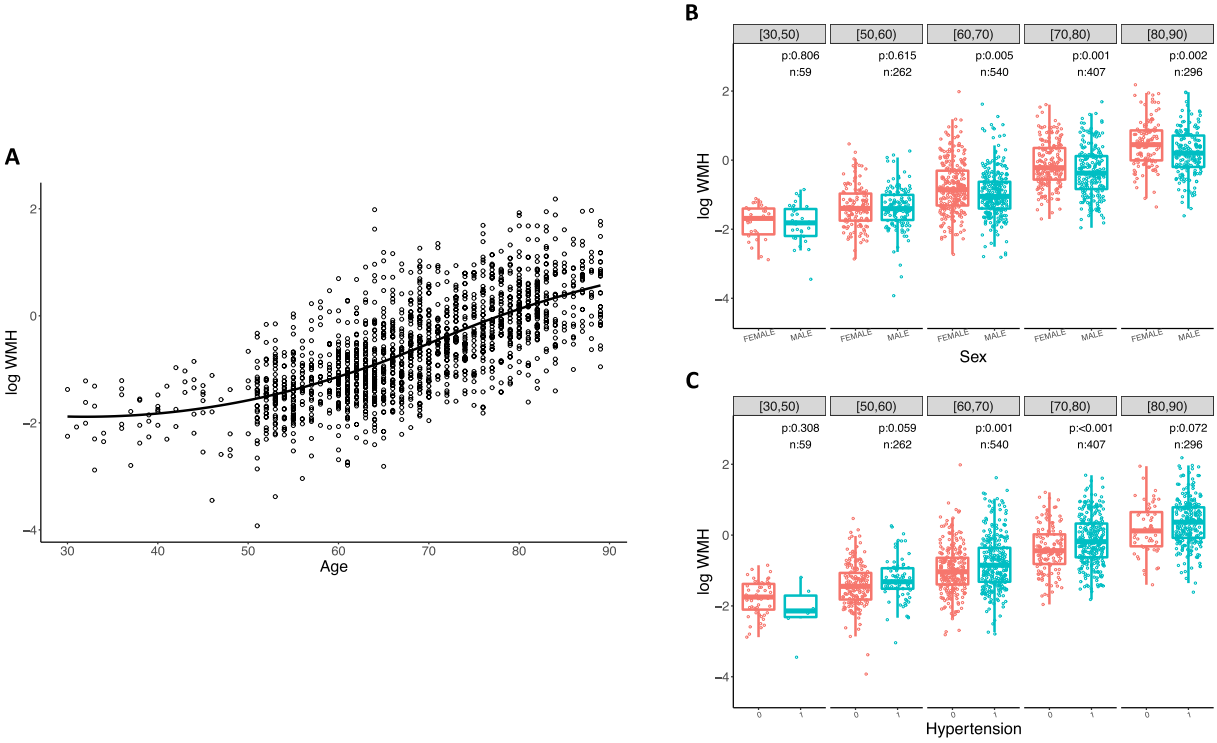

Fig. 1. Association between baseline WMH with (A) age, (B) sex, and (C) hypertension.

WMH between hypertensive and normotensive participants for ages 60–70 and 70–80 ($P < 0.01$).

In WMH models with all vascular risk factors including laboratory results shown in Table 1 as predictors, only presence of hypertension, increasing age, and female sex were significantly associated with both baseline and progression of WMH. The final models are shown in the regression models #1 & #2 ($P < 0.001$, Table 2). Neither diabetes nor hyperlipidemia showed a significant association with baseline WMH or WMH progression after adjusting for age, sex, and hypertension.

Table 2
Results from two regression (baseline) and two mixed models (progression) on WMH and WM health, Genu-FA.

Model #	Outcome	Predictors	Estimated effect size	SE	*P* value
# 1	Baseline WMH	Age	0.053	0.002	<0.001
		Male	−0.183	0.033	<0.001
		HTN	0.172	0.037	<0.001
# 2	WMH progression	Age	0.060	0.003	<0.001
		Male	−0.207	0.049	<0.001
		HTN	0.194	0.053	<0.001
# 3	Baseline Genu-FA	Age	−0.002	0.0001	<0.001
		Male	0.012	0.0022	<0.001
		HTN	−0.010	0.0024	<0.001
# 4	Genu-FA progression	Age	−0.002	0.0002	<0.001
		Male	0.013	0.0034	0.001
		HTN	−0.011	0.0036	0.003

WMH measurements are log-transformed. Higher WMH and lower Genu-FA represent poor brain health. HTN: Hypertension. Other potential variables were dropped out from the stepwise regression. 1564 participants are included in baseline analysis where 1396 are cognitively normal; 740 participants are included in the progression analysis, where 632 are cognitively normal.

3.2. Risk factors associated with baseline diffusion changes measured by DTI and its progression

We originally considered 12 WM tracts to measure WM health and to evaluate their usefulness in predicting WMH. Because FA of all the WM tracts are highly correlated, we considered FA of the genu of the corpus callosum (Genu-FA) which consists of thin fibers in the anterior part of the corpus callosum and has greater vulnerability to aging and neurovascular damage (Wassenaar et al., 2019). Previous data supports the use of Genu-FA as an important marker of cerebrovascular disease (Vemuri et al., 2018; Raghavan et al., 2020). We also considered three other tracts that were also predictive of WMH for comparison - FA of the splenium of the corpus callosum (Splenium-FA), FA of the body of the corpus callosum (Body-FA), and FA of the anterior limb of the internal capsule (ALIC-FA) as presented in Supplement material, section 3 sensitivity analysis.

In a model with Genu-FA as an outcome and vascular risk factors as predictors, only age, sex, and hypertension were associated with Genu-FA. As shown in Fig. 2A, Genu-FA decreases as age increases. Genu-FA significantly differed by sex in late-life with most significant findings in the 60–69 ($P < 0.001$), and 80–89 ($P = 0.007$) age groups (Fig. 2B). There were significant differences in Genu-FA between hypertensive and normotensive participants for all ages across late-life ($P \leq 0.006$) (Fig. 2C). Predictions of baseline and progressive WM integrity through Genu-FA are shown in Models #3 & #4 in Table 2. Older age, female sex, and hypertension were significantly associated with lower baseline and longitudinal Genu-FA in both models ($P < 0.001$, $P \leq 0.003$ respectively).

3.3. Genu-FA mediates the effect of hypertension and male sex on WMH

When we looked at the relationship between WMH and Genu-FA as illustrated in the scatterplot of Fig. 3A, we found high correlation between the two variables that increased with age. To further investigate the relationship between Genu-FA and WMH, we built two standardized regression models of WMH, controlling for age, sex, hypertension. In

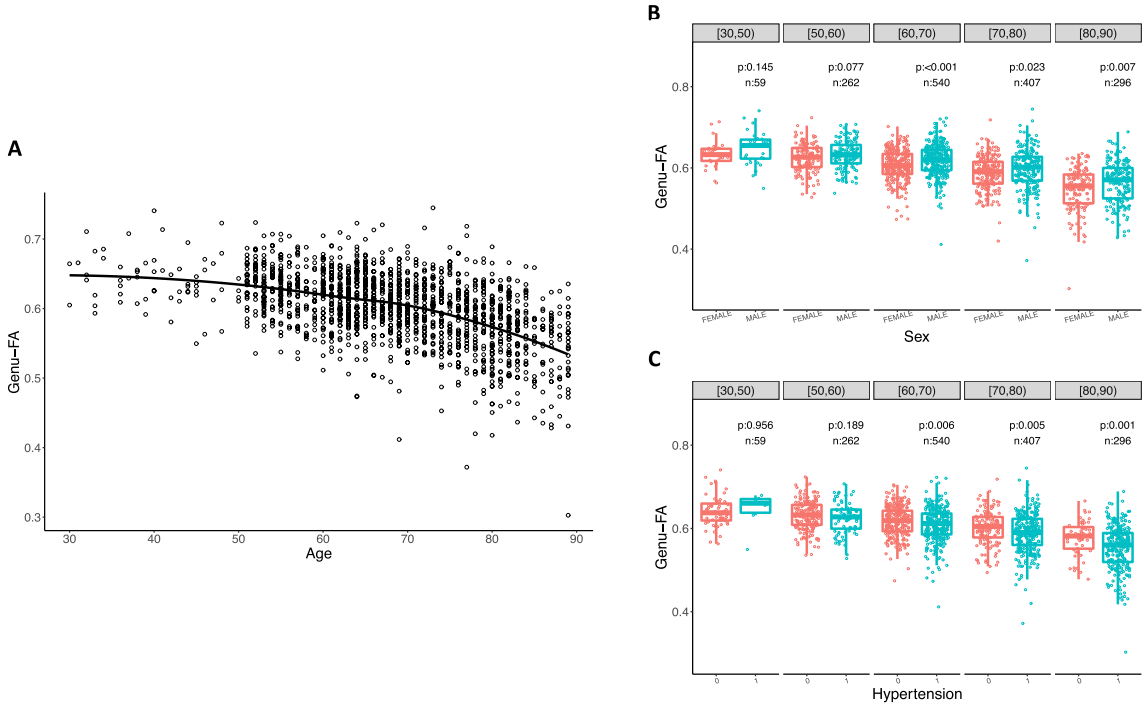

Fig. 2. Association between baseline WM health measured by Genu-FA with (A) age, (B) sex, and (C) hypertension.

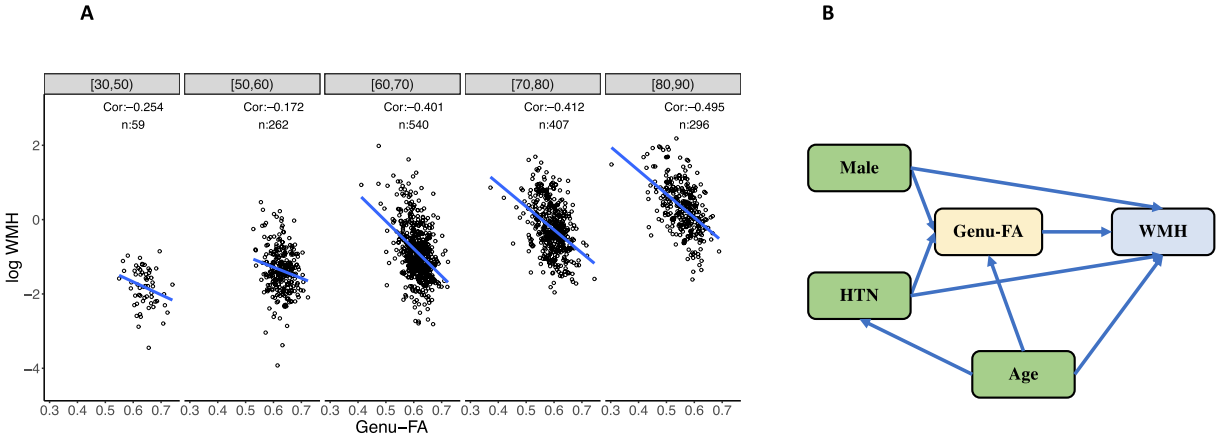

Fig. 3. **A** Relationship between baseline WMH and baseline Genu-FA in the pre-defined age groups. **B** shows the estimated local causal structure among age, sex, hypertension, WM health, and WMH, generated by the CSD algorithm.

model #5, we included Genu-FA but did not include in model #6 (Table 3). Our goal with this comparison was to understand the differences in standardized effect sizes between the two models. In model #5 from Table 3, Genu-FA was significantly associated with WMH (β = -0.29, P<0.0001). Compared to model #6, where Genu-FA was not included, the effect size from male sex and hypertension both dropped by approximately 40% (β = -0.1, 0.09 to −0.06, 0.06). This mediation analysis demonstrated that the effect of sex and hypertension was mediated by Genu-FA. The above conclusion was also confirmed in longitudinal analysis (Supplementary Table S1).

Fig. 3B shows the causal structure among the risk factors and WMH discovered by the CSD algorithm. A directed edge between two variables indicates a direct causal relationship. The relationships in the discovered graph are consistent with our previous finding as well as the mediation analysis.

Table 3
Results from two standardized regression models on WMH with and without controlling for WM health, Genu-FA.

Model #	Outcome	Predictors	Standardized effect size	SE	*P* value
# 5	Baseline WMH	Genu-FA	−0.29	0.020	<0.0001
		Age	0.52	0.020	<0.0001
		Male	−0.06	0.017	0.0003
		HTN	0.06	0.018	0.0004
# 6	Baseline WMH	Age	0.65	0.019	<0.0001
		Male	−0.10	0.018	<0.0001
		HTN	0.09	0.019	<0.0001

WMH measurements are log transformed before the standardized regression models.

3.4. Identifying factors related to the evolution of white matter hyperintensities

Based on previous findings, we studied the relationship between midlife risk factors and WMH. We included three midlife indicators, midlife cognitive activity, midlife physical activity, and smoking status. Table S2 shows that smoking status was strongly correlated with WMH (β = 0.05, P=0.0046), and midlife physical activity was significantly associated with WM health (Genu-FA) (β = 0.06, P<0.008) after adjusting for other predictors.

To study the effects of risk and protective factors on WMH, causal relationships, not merely associations, are needed. Therefore, we applied the CSD algorithm to all the sets of predictor variables. On the basis of the Fast Greedy Equivalence Search (Ramsey et al., 2017) (FGES), the causal structure discovered by the CSD algorithm is shown in Fig. 4. The complex relationships were described in one graph where an edge implies a direct causal effect. We then fitted multiple regression models to estimate the effect sizes for each edge.

While older age had an impact on all variables, male sex was associated with higher frequency of smokers, less cognitive activity, higher Genu-FA, and lower WMH. Physical and cognitive activity were highly correlated; there might exist other unobserved variables that are common between the two variables. Smoking (ever/never, measured up to midlife) was associated with greater later life WMH load, as has been observed in many other studies. The associations between hypertension and WM health/WMH that have been described in previous sections are also shown as a direct relationship in the graph. A key finding from the CSD graph was that greater physical activity in midlife was associated with healthier WM outcomes (mainly higher Genu-FA). The effect of greater physical activity had two pathways to better WM outcomes – 1) higher midlife physical activity was associated with higher Genu-FA (directly) and with lower WMH (through its effect on Genu-FA); 2) lower midlife physical activity was associated with higher BMI and higher BMI was associated with higher frequency of hypertension at the time of the scan which in turn contributed to lower WM health (lower Genu-FA and higher WMH).

The sex specific observations were interesting. Male sex was associated with higher frequency of smokers and had an impact on WM health through 1) direct impact on WMH and 2) through higher BMI contributing to greater frequency of hypertension. However, males in general had better WM outcomes as also confirmed by regression models suggesting that the net impact of male sex on WM outcomes was positive. While most of the relationships in the graph detected were plausible, there was one suggested relationship between higher cognitive activity and higher BMI that was not intuitive and should be interpreted with caution. Additional longitudinal data in future studies will be able to discern the relationship between physical activity, cognitive activity, and BMI which are highly inter-related and complex.

4. Discussion

In this large dataset of multi-modal imaging and clinical information, we investigated the relationships among WM health, WMH, and their risk factors. The major conclusion of the study was to identify pathways, particularly measuring early brain changes, to prevent WMH. Specifically, our main findings were: i) the effect of older age, hypertension, and female sex on greater WMH were mediated by diffusion changes seen on DTI; ii) midlife physical activity can aid in maintaining better microstructural health (and lower WMH) directly as well as indirectly through reduction of BMI which is associated with lower frequency of hypertension; iii) measuring Genu-FA can aid in prediction of WMH trajectories in the population; iv) further, the causal modeling of complex relationships identified key pathways related to the evolution of WMH.

4.1. Diffusion changes predictive of WMH trajectories

It has been widely shown that hypertension impacts WMH (Lane et al., 2019; Guo et al., 2009; Cox et al., 2019), and there is also emerging evidence that vascular risk factors are associated with WM damage (Wassenaar et al., 2019; Maillard et al., 2015; Hannawi et al., 2018). Our results from models 1 and 3 (Table 2) provide further evidence for the association between hypertension and WMH and its relationship with frontal WM (lower Genu-FA). Consistent with our findings, previous studies have reported associations of hypertension with lower FA in the genu of corpus callosum (de Groot et al., 2016; Pantoni, 2010). However, the actual mechanism underlying the association between hypertension and WM health is more complex and not clearly understood. Hypertension may cause vascular impairment leading to vascular remodeling and reduced vascular reserve, which may cause

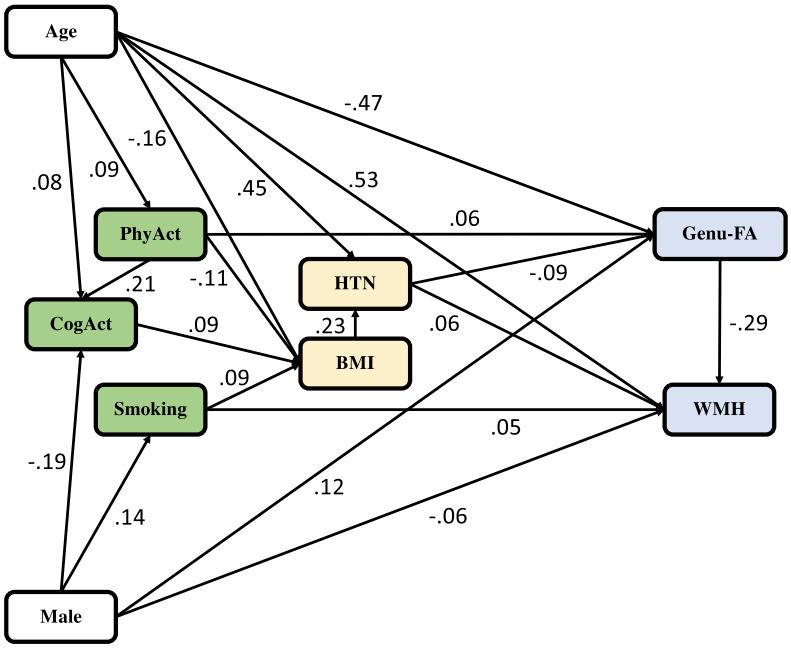

Fig. 4. The causal structure graph discovered using the CSD algorithm. The estimated standardized coefficients were labeled next to each edge.

arteriosclerosis, microatheroma, and microaneurysms. These processes result in reductions of blood flow, which can in turn cause myelin damage and gliosis (Wardlaw et al., 2013; Young et al., 2008) and the pathologies often observed as WMH on MRI (Arfanakis et al., 2020; Gyanwali et al., 2019). Our data also extends the past research from our group and others, showing that hypertension accelerated the progression of WMH (Lane et al., 2019; Lai et al., 2020; van Leijsen et al., 2018). In additional analyses, we observed that the impact of vascular health on WMH were mediated by WM health. Although hypertension was useful for prediction of future progression of WMH, WM microstructural integrity provides more information which is likely applicable earlier than WMH. Our findings are consistent with prior evidence showed that information captured by lower microstructural integrity was an independent predictor of conversion of normal appearing WM to WMH (Maillard et al., 2013; Khan et al., 2021; Vangberg et al., 2019; Vemuri et al., 2021). Furthermore, a previous study demonstrated distinct WM microstructural patterns with increasing WMH load even before the formation of lesions and pleiotropic effects, suggesting WM changes as the early measure of WMH (Alqarni et al., 2021). Previous longitudinal studies also have shown that microstructural WM alterations measured by FA and MD are correlated with future WMH (Cees De Groot et al., 2000; Maillard et al., 2013). More recently, we also found a stronger association between Genu-FA and WMH that lend support of the frontal WM damage due to systemic vascular health prior to WMH (Sachdev et al., 2009). However, there was no established link for a mediating effect of Genu-FA on WMH that makes these study findings more unique. This new finding might indicate the importance of targeting early changes in WM as a predictor of future changes of WMH in middle-aged and older adults. These findings also support the usefulness of DTI in clinical prevention trials targeting modifiable vascular risk factors and the reduction of WMH.

4.2. Sex differences in WM health

The current study also showed a sex-specific association with microstructural integrity of WM and found a greater vulnerability in females with greater baseline WMH burden and progressive WMH. These findings extend our past research (Fatemi et al., 2018; Lane et al., 2019) and several others (van den Heuvel et al., 2004; Sachdev et al., 2016; Miller et al., 2013), suggesting that sex is an important factor contributing to WMH. The possible explanations include genetic and hormonal factors, sexual dimorphism in WM microstructure, and their influence on CVD. A higher genetic heritability of WMH has been shown in women compared to men (Miller et al., 2020). The major hormonal changes in women are associated with pregnancy and menopause. Studies have suggested the link between hypertensive pregnancy disorders such as preeclampsia and WMH (Cook et al., 2002; Liu et al., 2009). It is also possible that reduction in estrogen after menopause may have an influence and suggested that hormone replacement therapy might protect the WM integrity (Liu et al., 2009; Jayachandran et al., 2020; Zeydan et al., 2019). However, a recent study in women of the Kronos Early Estrogen Prevention Study failed to reveal any significant association of menopausal hormone treatments with WMH (Coutinho, 2014). Although studies often considered a possible association of bilateral oophorectomy with WMH formation and progression (Cook et al., 2002), no significant evidence is available yet (Sullivan et al., 2010). Evidence also suggested that a higher frequency of arterial stiffness in women might lead to increased WMH burden through cerebrovascular remodeling (Westerhausen et al., 2003).

Interestingly, the male effect on WMH was mediated through better WM health, suggesting that organization of WM fiber tracts are relatively preserved in men. The mediating effect of higher Genu-FA contributing to lower WMH in men has not been reported previously, to our knowledge. However, prior studies of the corpus callosum revealed inconsistent findings in association with sex in which some reported higher FA in men (Kanaan et al., 2012; Oh et al., 2007), others found higher FA in women (Nuñez et al., 2000; Cerghet et al., 2006). Animal studies have shown that there is a greater proportion (and area) of myelinated fibers in males than females in the corpus callosum (Debette et al., 2011), which could explain greater white matter reserve in men to ongoing damage. Another possible mechanism may be the different protein composition in myelin sheaths and the greater turnover of oligodendrocytes observed in females (Durhan et al., 2016). Further research is warranted to investigate the sexual dimorphism of WM health and WMH.

4.3. Factors driving WM changes

The local relationships between midlife modifiers and WM measurements extracted from Fig. 4 are shown in Fig. 5. Consistent with previous findings (Gray et al., 2020; Fleischman et al., 2015), we found smoking is associated with WMH which were confirmed by both the regression and CSD analyses. These associations between cigarette exposure and WMH were also well established in two large samples from the UK Biobank (Maillard et al., 2015; Vesperman et al., 2018). Our findings further provide evidence for an association between smoking effects and poorer WM integrity. As expected, there was an association between smoking and lower Genu-FA, these anterior fibers are most susceptible to normal and neurovascular aging (Wassenaar et al., 2019; Maillard et al., 2015). In addition, midlife physical activity showed an indirect association with WMH through the path of WM health. There are also reports on the short and long term effects of physical activity on brain health. Evidence suggests that higher levels of physical activity attenuate the amount of WMH in middle aged and older adults (Palta et al., 2021; Tarumi et al., 2021). A recent study from Atherosclerosis Risk in Communities (ARIC) suggests that greater levels of midlife and late-life physical activity may reduce cerebrovascular lesions in late-life (Wartolowska and Webb, 2021) and hence aid in preventing cognitive decline. Although, there is very little evidence on the effect of midlife physical activity on midlife WM integrity, a more recent study suggests that midlife aerobic exercise may prevent or slow down the detrimental age-related WM fiber integrity degradation (Garnier-Crussard et al., 2020). They also demonstrated greater FA in the genu, superior longitudinal fasciculus, and uncinate fasciculus in middle aged aerobically trained adults compared to middle aged sedentary.

It is also well known that hypertension affects WMH (Lane et al., 2019; van Leijsen et al., 2018; Lampe et al., 2019; Griffanti et al., 2018), however, the indirect pathway through BMI was not established before. Interestingly, BMI association with WMH has been reported (Griffanti et al., 2018; Lampe et al., 2019), with higher volumes in women, especially in the deep WMH (van den Heuvel et al., 2004). In the present work, using a causal model, without any prior information, the model identified an indirect relationship with WMH. Further investigations are needed to confirm this hypothesized mechanism and better establish the interrelationships. Altogether, our data revealed the neuroprotective mechanism by which better midlife physical and cognitive activity and not smoking may protect against cerebrovascular sequelae. Further, we provided evidence that DTI based measures may be appropriate as surrogate measures of WMH for clinical trials targeting vascular risk factors.

While studying the midlife modifiers of WMH, we implemented causal structure discovery to generate the causal graph among risk factors and WMH. The discovered graph was then compared with the results from traditional statistical analyses. The workflow that embedded CSD method provides benefits in the following ways: (1) Under a set of assumptions, the relationships discovered from CSD methods have a causal interpretation. For example, a causal relationship from X to Y has the interpretation that changes in X lead to changes in Y. We also note that these causal conclusions are potential hypotheses that still need to be validated with further experiments; (2) When the goal of the study is not merely predicting the outcome, knowing the structure among risk factors helps understand the underlying biological

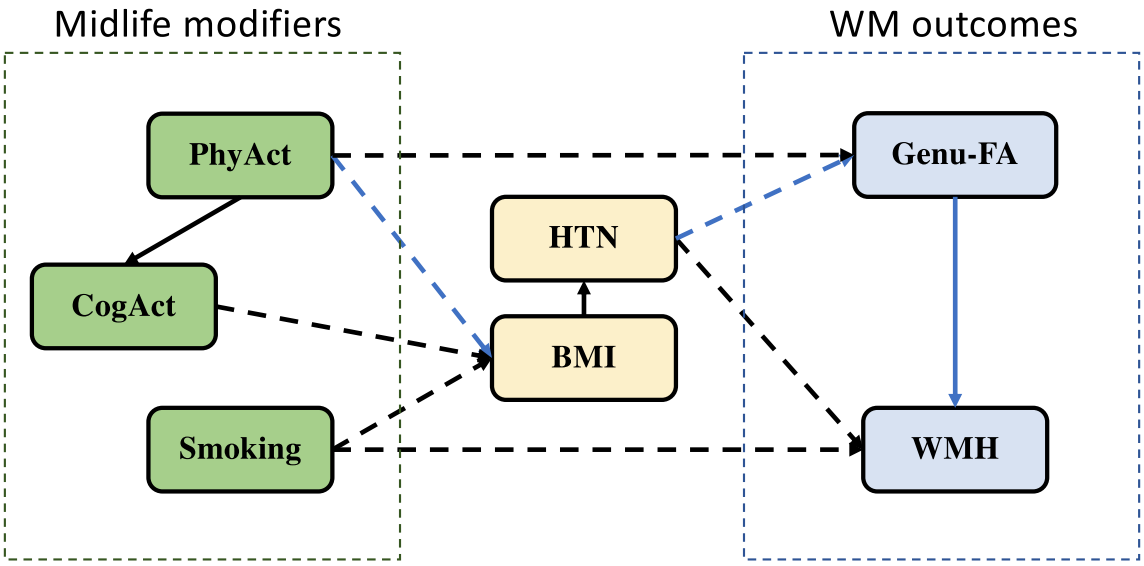

Fig. 5. Important Relationships between midlife modifiers and WMH/WM health discovered by the CSD algorithm Blue and black arrows represent negative and positive (respective) causal relationships from the source to the target and the dashed arrow represents a statistically significant relationship with standardized effect size<0.2, while solid arrows represent standardized effect sizes at least 0.2.

mechanism with reasonably high accuracy (Shen et al., 2020); (3) In our current workflow, the CSD model was mainly used for validating the conclusion from well-established traditional methods. However, it can also be used for hypothesis generation. We can design the regression analyses based on the causal graph obtained through CSD methods. The workflow of how the CSD model was used may change the way of investigating the relationship between risk factors and targets of interests. The goal of the study is not to study all variables that influence WM outcomes. In our study, the framework is focused on finding early brain measures and early (risk and protective) factors that influence WMH trajectories. We tested this framework by modeling brain measures as outcomes (i.e. WMH and DTI) using regression models and also modeled the complex relationships using CSD with all factors in a single model. Our goal was to generate test hypotheses but not design treatment trials. Given the large number of variables, causal analysis can be leveraged to identify critical variables for further rigorous investigation. The method allows identification of key variables that can be potentially targeted for treatment trials.

*4.4. Strengths and **Limitations***

The study has several strengths. First, the availability of large data set with diffusion, FLAIR, and T1 weighted MRI across the adult lifespan enabled us to study their complex causal relationship. Second, the information on the vascular risk factors based on their medical records through REP was crucial, although none of laboratory values showed significance. The third strength was the newly implemented workflow, which by combining the CSD methods with regression analysis, may improve the design of prevention trials.

The study also has some limitations. First, although we considered the longitudinal aspect, only 10 percent of participants had 3 or more observations, and more than half of participants have one available visit. To make use of all available data, we conducted pairs of analyses, one regression analysis for baseline observations, and one mixed effect analysis for longitudinal data. Ideally, longitudinal data can provide more knowledge when studying the mixed effect, and we have shown before that the temporal information naturally provided by the longitudinal data also helps the CSD method to achieve higher accuracy[84]. Second, we only considered the global measure of WMH and did not consider regional variability. Third, relatively shorter longitudinal observation intervals. Fourth, though we did extensive bootstrapping to confirm our study findings, we acknowledge that the uniqueness of this dataset with extensive clinical and imaging data limits our ability to replicate this in an independent dataset. Fourth, a possible limitation may be that many laboratory values were under control by medications, so they are likely to become less predictive compared with the disease diagnosis code. Fifth, the smaller sample size in the cognitively impaired participants reflects the population-based sample. In the future, we would be able to extend the study to a large sample to investigate the complex interplay between regional measures of WM health and WMH.

5. Conclusions

The present study demonstrated a significant age, sex, and hypertension association with WMH. The relationship between vascular factors and WMH can be better explained by early changes in WM microstructural integrity. The midlife modifiers emerged as important components of WM health. Hence midlife may be the relevant window for prevention of late-life WMHs and measuring microstructural integrity using DTI can aid in better design and monitoring of prevention trials.

6. Data and Materials availability

Qualified researcher can make reasonable request of data from Mayo Clinic Study of Aging.

Author Contributions

X.S., S.M., G.S., and P.V. conceived and designed the study. All authors participated in data collection and/or analysis. X.S., S.R., P.V., G. S., S.M., S.P., T.L., R.R. drafted, reviewed, and edited the manuscript. All authors read and approved the final manuscript.

Declaration of Competing Interest

The authors declare that they have no known competing financial interests or personal relationships that could have appeared to influence the work reported in this paper.

Acknowledgments and Funding

This work was supported by NIH grants R01 NS097495 (PI: Vemuri), U01 AG06786 (PI: Petersen/Mielke/Jack), R01 AG56366 (PI: Vemuri), P50 AG16574 (PI: Petersen), R37 AG11378 (PI: Jack), R01 AG41851 (PIs: Jack and Knopman); the Gerald and Henrietta Rauenhorst Foundation grant, Alzheimer's Drug Discovery Foundation (ADDF), the Alexander Family Alzheimer's Disease Research Professorship of the Mayo Foundation, Liston Award, Elsie and Marvin Dekelboum Family Foundation, Schuler Foundation, Opus building NIH grant C06 RR018898, and was made possible by Rochester Epidemiology Project (R01 AG34676).

Appendix A. Supplementary data

Supplementary data to this article can be found online at https://doi.org/10.1016/j.nicl.2022.103077.

References

Whitman GT, Tang Y, Lin A, Baloh RW. A prospective study of cerebral white matter abnormalities in older people with gait dysfunction. Neurology. 2001;57(6):990-994.

Cees De Groot, J., De Leeuw, F.-E., Oudkerk, M., Van Gijn, J., Hofman, A., Jolles, J., Breteler, M.M.B., 2000. Cerebral white matter lesions and cognitive function: the Rotterdam Scan Study. Ann Neurol. 47 (2), 145–151.

S. Debette S, Markus HS. The clinical importance of white matter hyperintensities on brain magnetic resonance imaging: systematic review and meta-analysis. *Bmj.* 2010; 341:c3666.

Scharf, E.L., Graff-Radford, J., Przybelski, S.A., Lesnick, T.G., Mielke, M.M., Knopman, D. S., Preboske, G.M., Schwarz, C.G., Senjem, M.L., Gunter, J.L., Machulda, M., Kantarci, K., Petersen, R.C., Jack, C.R., Vemuri, P., 2019. Cardiometabolic Health and Longitudinal Progression of White Matter Hyperintensity: The Mayo Clinic Study of Aging. Stroke. 50 (11), 3037–3044.

Habes, M., Erus, G., Toledo, J.B., Zhang, T., Bryan, N., Launer, L.J., Rosseel, Y., Janowitz, D., Doshi, J., Van der Auwera, S., von Sarnowski, B., Hegenscheid, K., Hosten, N., Homuth, G., Völzke, H., Schminke, U., Hoffmann, W., Grabe, H.J., Davatzikos, C., 2016. White matter hyperintensities and imaging patterns of brain ageing in the general population. Brain. 139 (4), 1164–1179.

Gottesman, R.F., Coresh, J., Catellier, D.J., Sharrett, A.R., Rose, K.M., Coker, L.H., Shibata, D.K., Knopman, D.S., Jack, C.R., Mosley, T.H., 2010. Blood pressure and white-matter disease progression in a biethnic cohort: Atherosclerosis Risk in Communities (ARIC) study. Stroke. 41 (1), 3–8.

Godin, O., Tzourio, C., Maillard, P., Mazoyer, B., Dufouil, C., 2011. Antihypertensive treatment and change in blood pressure are associated with the progression of white matter lesion volumes: the Three-City (3C)-Dijon Magnetic Resonance Imaging Study. Circulation. 123 (3), 266–273.

Fatemi F, Kantarci K, Graff-Radford J, et al. Sex differences in cerebrovascular pathologies on FLAIR in cognitively unimpaired elderly. *Neurology.* 2018;90(6): e466-e473.

Maillard, P., Carmichael, O., Harvey, D., Fletcher, E., Reed, B., Mungas, D., DeCarli, C., 2013. FLAIR and diffusion MRI signals are independent predictors of white matter hyperintensities. AJNR Am J Neuroradiol. 34 (1), 54–61.

Maniega, S.M., Valdés Hernández, M.C., Clayden, J.D., Royle, N.A., Murray, C., Morris, Z., Aribisala, B.S., Gow, A.J., Starr, J.M., Bastin, M.E., Deary, I.J., Wardlaw, J.M., 2015. White matter hyperintensities and normal-appearing white matter integrity in the aging brain. Neurobiol Aging. 36 (2), 909–918.

Pearl, J., 2009. Causality. Cambridge University Press, Cambridge.

Li, Y., Torralba, A., Anandkumar, A., Fox, D., Garg, A., 2020. Causal Discovery in Physical Systems from Videos. NeurIPS.

Anker, J.J., Kummerfeld, E., Rix, A., Burwell, S.J., Kushner, M.G., 2019. Causal Network Modeling of the Determinants of Drinking Behavior in Comorbid Alcohol Use and Anxiety Disorder. Alcoholism: Clinical and Experimental Research. 43 (1), 91–97.

Ebert-Uphoff, I., Deng, Y., 2012. Causal Discovery for Climate Research Using Graphical Models. Journal of Climate. 25 (17), 5648–5665.

Rocca, W.A., Yawn, B.P., St Sauver, J.L., Grossardt, B.R., Melton 3rd., L.J., 2012. History of the Rochester Epidemiology Project: half a century of medical records linkage in a US population. Mayo Clinic proceedings. 87 (12), 1202–1213.

St Sauver, J.L., Grossardt, B.R., Yawn, B.P., Melton, L.J., Pankratz, J.J., Brue, S.M., Rocca, W.A., 2012. Data resource profile: the Rochester Epidemiology Project (REP) medical records-linkage system. Int J Epidemiol. 41 (6), 1614–1624.

Roberts, R.O., Geda, Y.E., Knopman, D.S., Cha, R.H., Pankratz, V.S., Boeve, B.F., Ivnik, R. J., Tangalos, E.G., Petersen, R.C., Rocca, W.A., 2008. The Mayo Clinic Study of Aging: design and sampling, participation, baseline measures and sample characteristics. Neuroepidemiology. 30 (1), 58–69.

Petersen, R.C., Roberts, R.O., Knopman, D.S., Geda, Y.E., Cha, R.H., Pankratz, V.S., Boeve, B.F., Tangalos, E.G., Ivnik, R.J., Rocca, W.A., 2010. Prevalence of mild cognitive impairment is higher in men. The Mayo Clinic Study of Aging. Neurology. 75 (10), 889–897.

Graff-Radford, J., Arenaza-Urquijo, E.M., Knopman, D.S., Schwarz, C.G., Brown, R.D., Rabinstein, A.A., Gunter, J.L., Senjem, M.L., Przybelski, S.A., Lesnick, T., Ward, C., Mielke, M.M., Lowe, V.J., Petersen, R.C., Kremers, W.K., Kantarci, K., Jack, C.R., Vemuri, P., 2019. White matter hyperintensities: relationship to amyloid and tau burden. Brain : a journal of neurology. 142 (8), 2483–2491.

Reid, R.I.N.Z., Schwarz, C.G., et al., 2018. Diffusion specific segmentation: skull stripping with diffusion MRI data alone. Springer, Cham.

Veraart, J., Novikov, D.S., Christiaens, D., Ades-Aron, B., Sijbers, J., Fieremans, E., 2016. Denoising of diffusion MRI using random matrix theory. NeuroImage. 142, 394–406.

Andersson, J.L.R., Graham, M.S., Zsoldos, E., Sotiropoulos, S.N., 2016. Incorporating outlier detection and replacement into a non-parametric framework for movement and distortion correction of diffusion MR images. NeuroImage. 141, 556–572.

Kellner, E., Dhital, B., Kiselev, V.G., Reisert, M., 2016. Gibbs-ringing artifact removal based on local subvoxel-shifts. Magnetic resonance in medicine. 76 (5), 1574–1581.

Koay, C.G., Özarslan, E., Basser, P.J., 2009. A signal transformational framework for breaking the noise floor and its applications in MRI. Journal of Magnetic Resonance 197 (2), 108–119.

Garyfallidis, E., Brett, M., Amirbekian, B., Rokem, A., van der Walt, S., Descoteaux, M., Nimmo-Smith, I., 2014. Dipy, a library for the analysis of diffusion MRI data. Frontiers in neuroinformatics. 8.

Avants, B.B., Tustison, N.J., Song, G., Cook, P.A., Klein, A., Gee, J.C., 2011. A reproducible evaluation of ANTs similarity metric performance in brain image registration. NeuroImage. 54 (3), 2033–2044.

Oishi, K., Faria, A., Jiang, H., Li, X., Akhter, K., Zhang, J., Hsu, J.T., Miller, M.I., van Zijl, P.C.M., Albert, M., Lyketsos, C.G., Woods, R., Toga, A.W., Pike, G.B., Rosa-Neto, P., Evans, A., Mazziotta, J., Mori, S., 2009. Atlas-based whole brain white matter analysis using large deformation diffeomorphic metric mapping: application to normal elderly and Alzheimer's disease participants. NeuroImage. 46 (2), 486–499.

Roberts, R.O., Knopman, D.S., Przybelski, S.A., Mielke, M.M., Kantarci, K., Preboske, G. M., Senjem, M.L., Pankratz, V.S., Geda, Y.E., Boeve, B.F., Ivnik, R.J., Rocca, W.A., Petersen, R.C., Jack, C.R., 2014. Association of type 2 diabetes with brain atrophy and cognitive impairment. Neurology. 82 (13), 1132–1141.

Vemuri, P., Lesnick, T.G., Przybelski, S.A., Knopman, D.S., Roberts, R.O., Lowe, V.J., Kantarci, K., Senjem, M.L., Gunter, J.L., Boeve, B.F., Petersen, R.C., Jack, C.R., 2012. Effect of lifestyle activities on Alzheimer disease biomarkers and cognition. Annals of neurology. 72 (5), 730–738.

Wardlaw, J.M., Chappell, F.M., Valdés Hernández, M.D.C., Makin, S.D.J., Staals, J., Shuler, K., Thrippleton, M.J., Armitage, P.A., Muñoz-Maniega, S., Heye, A.K., Sakka, E., Dennis, M.S., 2017. White matter hyperintensity reduction and outcomes after minor stroke. Neurology. 89 (10), 1003–1010.

VanderWeele, T.J., 2016. Mediation Analysis: A Practitioner's Guide. Annual Review of Public Health. 37 (1), 17–32.

Spirtes, P., Clark, G., Scheines, R., 2000. Causation, Prediction, and Search. The MIT Press.

Glymour, C., Zhang, K., Spirtes, P., 2019. Review of Causal Discovery Methods Based on Graphical Models. Frontiers in Genetics. 10 (524).

Ramsey, J., Glymour, M., Sanchez-Romero, R., Glymour, C., 2017. A million variables and more: the Fast Greedy Equivalence Search algorithm for learning high-dimensional graphical causal models, with an application to functional magnetic resonance images. International Journal of Data Science and Analytics. 3 (2), 121–129.

Wassenaar, T.M., Yaffe, K., van der Werf, Y.D., Sexton, C.E., 2019. Associations between modifiable risk factors and white matter of the aging brain: insights from diffusion tensor imaging studies. Neurobiology of aging. 80, 56–70.

Vemuri, P., Lesnick, T.G., Przybelski, S.A., Graff-Radford, J., Reid, R.I., Lowe, V.J., Zuk, S.M., Senjem, M.L., Schwarz, C.G., Gunter, J.L., Kantarci, K., Machulda, M.M., Mielke, M.M., Petersen, R.C., Knopman, D.S., Jack, C.R., 2018. Development of a cerebrovascular magnetic resonance imaging biomarker for cognitive aging. Annals of neurology. 84 (5), 705–716.

Raghavan, S., Przybelski, S.A., Reid, R.I., Graff-Radford, J., Lesnick, T.G., Zuk, S.M., Knopman, D.S., Machulda, M.M., Mielke, M.M., Petersen, R.C., Jack, C.R., Vemuri, P., 2020. Reduced fractional anisotropy of the genu of the corpus callosum as a cerebrovascular disease marker and predictor of longitudinal cognition in MCI. Neurobiol Aging. 96, 176–183.

Lane, C.A., Barnes, J., Nicholas, J.M., Sudre, C.H., Cash, D.M., Parker, T.D., Malone, I.B., Lu, K., James, S.-N., Keshavan, A., Murray-Smith, H., Wong, A., Buchanan, S.M., Keuss, S.E., Gordon, E., Coath, W., Barnes, A., Dickson, J., Modat, M., Thomas, D., Crutch, S.J., Hardy, R., Richards, M., Fox, N.C., Schott, J.M., 2019. Associations between blood pressure across adulthood and late-life brain structure and pathology in the neuroscience substudy of the 1946 British birth cohort (Insight 46): an epidemiological study. Lancet Neurol. 18 (10), 942–952.

Guo, X., Pantoni, L., Simoni, M., Bengtsson, C., Björkelund, C., Lissner, L., Gustafson, D., Skoog, I., 2009. Blood pressure components and changes in relation to white matter lesions: a 32-year prospective population study. Hypertension. 54 (1), 57–62.

Cox, S.R., Lyall, D.M., Ritchie, S.J., Bastin, M.E., Harris, M.A., Buchanan, C.R., Fawns-Ritchie, C., Barbu, M.C., de Nooij, L., Reus, L.M., Alloza, C., Shen, X., Neilson, E., Alderson, H.L., Hunter, S., Liewald, D.C., Whalley, H.C., McIntosh, A.M., Lawrie, S. M., Pell, J.P., Tucker-Drob, E.M., Wardlaw, J.M., Gale, C.R., Deary, I.J., 2019. Associations between vascular risk factors and brain MRI indices in UK Biobank. Eur Heart J. 40 (28), 2290–2300.

Maillard, P., Carmichael, O.T., Reed, B., Mungas, D., DeCarli, C., 2015. Cooccurrence of vascular risk factors and late-life white-matter integrity changes. Neurobiol Aging. 36 (4), 1670–1677.

Hannawi, Y., Yanek, L.R., Kral, B.G., Vaidya, D., Becker, L.C., Becker, D.M., Nyquist, P. A., 2018. Hypertension Is Associated with White Matter Disruption in Apparently Healthy Middle-Aged Individuals. AJNR Am J Neuroradiol. 39 (12), 2243–2248.
de Groot, M., Cremers, L.G.M., Ikram, M.A., Hofman, A., Krestin, G.P., van der Lugt, A., Niessen, W.J., Vernooij, M.W., 2016. White Matter Degeneration with Aging: Longitudinal Diffusion MR Imaging Analysis. Radiology. 279 (2), 532–541.
Pantoni, L., 2010. Cerebral small vessel disease: from pathogenesis and clinical characteristics to therapeutic challenges. Lancet Neurol. 9 (7), 689–701.
Wardlaw, J.M., Smith, C., Dichgans, M., 2013. Mechanisms of sporadic cerebral small vessel disease: insights from neuroimaging. Lancet Neurol. 12 (5), 483–497.
Young, V.G., Halliday, G.M., Kril, J.J., 2008. Neuropathologic correlates of white matter hyperintensities. Neurology. 71 (11), 804–811.
Arfanakis, K., Evia, A.M., Leurgans, S.E., Cardoso, L.F.C., Kulkarni, A., Alqam, N., Lopes, L.F., Vieira, D., Bennett, D.A., Schneider, J.A., Flanagan, M., 2020. Neuropathologic Correlates of White Matter Hyperintensities in a Community-Based Cohort of Older Adults. J Alzheimers Dis. 73 (1), 333–345.
Gyanwali, B., Shaik, M.A., Tan, B.Y., Venketasubramanian, N., Chen, C., Hilal, S., 2019. Risk Factors for and Clinical Relevance of Incident and Progression of Cerebral Small Vessel Disease Markers in an Asian Memory Clinic Population. J Alzheimers Dis. 67 (4), 1209–1219.
Lai, Y., Jiang, C., Du, X., Sang, C., Guo, X., Bai, R., Tang, R., Dong, J., Ma, C., 2020. Effect of intensive blood pressure control on the prevention of white matter hyperintensity: Systematic review and meta-analysis of randomized trials. J Clin Hypertens (Greenwich). 22 (11), 1968–1973.
van Leijsen, E.M.C., Bergkamp, M.I., van Uden, I.W.M., Ghafoorian, M., van der Holst, H. M., Norris, D.G., Platel, B., Tuladhar, A.M., de Leeuw, F.-E., 2018. Progression of White Matter Hyperintensities Preceded by Heterogeneous Decline of Microstructural Integrity. Stroke. 49 (6), 1386–1393.
Khan, W., Khlif, M.S., Mito, R., Dhollander, T., Brodtmann, A., 2021. Investigating the microstructural properties of normal-appearing white matter (NAWM) preceding conversion to white matter hyperintensities (WMHs) in stroke survivors. NeuroImage. 232, 117839.
Vangberg TR, Eikenes L, Håberg AK. The effect of white matter hyperintensities on regional brain volumes and white matter microstructure, a population-based study in HUNT. *NeuroImage*. 2019;203:116158.
Vemuri, P., Graff-Radford, J., Lesnick, T.G., Przybelski, S.A., Reid, R.I., Reddy, A.L., Lowe, V.J., Mielke, M.M., Machulda, M.M., Petersen, R.C., Knopman, D.S., Jack, C. R., 2021. White matter abnormalities are key components of cerebrovascular disease impacting cognitive decline. *Brain*. Communications. 3 (2).
Alqarni, A., Jiang, J., Crawford, J.D., Koch, F., Brodaty, H., Sachdev, P., Wen, W., 2021. Sex differences in risk factors for white matter hyperintensities in non-demented older individuals. Neurobiol Aging. 98, 197–204.
Sachdev, P.S., Parslow, R., Wen, W., Anstey, K.J., Easteal, S., 2009. Sex differences in the causes and consequences of white matter hyperintensities. Neurobiol Aging. 30 (6), 946–956.
van den Heuvel, D.M.J., Admiraal-Behloul, F., ten Dam, V.H., Olofsen, H., Bollen, E.L.E. M., Murray, H.M., Blauw, G.J., Westendorp, R.G.J., de Craen, A.J.M., van Buchem, M.A., 2004. Different progression rates for deep white matter hyperintensities in elderly men and women. Neurology. 63 (9), 1699–1701.
Sachdev, P.S., Thalamuthu, A., Mather, K.A., Ames, D., Wright, M.J., Wen, W., Bowden, J., Lee, T., Brodaty, H., Crawford, J., Duckworth, T., Kang, K., Garden, N., Martin, N., Lemmon, C., 2016. White Matter Hyperintensities Are Under Strong Genetic Influence. Stroke. 47 (6), 1422–1428.
Miller, V.M., Garovic, V.D., Kantarci, K., Barnes, J.N., Jayachandran, M., Mielke, M.M., Joyner, M.J., Shuster, L.T., Rocca, W.A., 2013. Sex-specific risk of cardiovascular disease and cognitive decline: pregnancy and menopause. Biol Sex Differ. 4 (1), 6.
Miller, V.M., Jayachandran, M., Barnes, J.N., Mielke, M.M., Kantarci, K., Rocca, W.A., 2020. Risk factors of neurovascular ageing in women. J Neuroendocrinol. 32 (1), e12777.
Cook, I.A., Morgan, M.L., Dunkin, J.J., David, S., Witte, E., Lufkin, R., Abrams, M., Rosenberg, S., Leuchter, A.F., 2002. Estrogen replacement therapy is associated with less progression of subclinical structural brain disease in normal elderly women: a pilot study. Int J Geriatr Psychiatry. 17 (7), 610–618.
Liu, Y.-Y., Hu, L., Ji, C., Chen, D.-W., Shen, X.i., Yang, N., Yue, Y., Jiang, J.-M., Hong, X., Ge, Q.-S., Zuo, P.-P., 2009. Effects of hormone replacement therapy on magnetic resonance imaging of brain parenchyma hyperintensities in postmenopausal women. Acta Pharmacol Sin. 30 (7), 1065–1070.
Jayachandran, M., Lahr, B.D., Bailey, K.R., Miller, V.M., Kantarci, K., 2020. Menopausal hormone therapy, blood thrombogenicity, and development of white matter hyperintensities in women of the Kronos Early Estrogen Prevention Study. Menopause. 27 (3), 305–310.
Zeydan, B., Tosakulwong, N., Schwarz, C.G., Senjem, M.L., Gunter, J.L., Reid, R.I., Gazzuola Rocca, L., Lesnick, T.G., Smith, C.Y., Bailey, K.R., Lowe, V.J., Roberts, R.O., Jack, C.R., Petersen, R.C., Miller, V.M., Mielke, M.M., Rocca, W.A., Kantarci, K., 2019. Association of Bilateral Salpingo-Oophorectomy Before Menopause Onset With Medial Temporal Lobe Neurodegeneration. JAMA Neurol. 76 (1), 95.
Coutinho, T., 2014. Arterial stiffness and its clinical implications in women. Can J Cardiol. 30 (7), 756–764.
Sullivan, E.V., Rohlfing, T., Pfefferbaum, A., 2010. Quantitative fiber tracking of lateral and interhemispheric white matter systems in normal aging: relations to timed performance. Neurobiol Aging. 31 (3), 464–481.
Westerhausen, R., Walter, C., Kreuder, F., Wittling, R.A., Schweiger, E., Wittling, W., 2003. The influence of handedness and gender on the microstructure of the human corpus callosum: a diffusion-tensor magnetic resonance imaging study. Neurosci Lett. 351 (2), 99–102.
Kanaan, R.A., Allin, M., Picchioni, M., Barker, G.J., Daly, E., Shergill, S.S., Woolley, J., McGuire, P.K., Gong, Q., 2012. Gender differences in white matter microstructure. PLoS One. 7 (6), e38272.
Oh, J.S., Song, I.C., Lee, J.S., Kang, H., Park, K.S., Kang, E., Lee, D.S., 2007. Tractography-guided statistics (TGIS) in diffusion tensor imaging for the detection of gender difference of fiber integrity in the midsagittal and parasagittal corpora callosa. Neuroimage. 36 (3), 606–616.
Nuñez, J.L., Nelson, J., Pych, J.C., Kim, J.H., Juraska, J.M., 2000. Myelination in the splenium of the corpus callosum in adult male and female rats. Brain Res Dev Brain Res. 120 (1), 87–90.
Cerghet, M., Skoff, R.P., Bessert, D., Zhang, Z., Mullins, C., Ghandour, M.S., 2006. Proliferation and death of oligodendrocytes and myelin proteins are differentially regulated in male and female rodents. J Neurosci. 26 (5), 1439–1447.
Debette, S., Seshadri, S., Beiser, A., Au, R., Himali, J.J., Palumbo, C., Wolf, P.A., DeCarli, C., 2011. Midlife vascular risk factor exposure accelerates structural brain aging and cognitive decline. Neurology. 77 (5), 461–468.
Durhan, G., Diker, S., Has, A.C., Karakaya, J., Tuncer Kurne, A., Oguz, K.K., 2016. Influence of cigarette smoking on white matter in patients with clinically isolated syndrome as detected by diffusion tensor imaging. Diagn Interv Radiol. 22 (3), 291–296.
Gray, J.C., Thompson, M., Bachman, C., Owens, M.M., Murphy, M., Palmer, R., 2020. Associations of cigarette smoking with gray and white matter in the UK Biobank. Neuropsychopharmacology. 45 (7), 1215–1222.
Fleischman, D.A., Yang, J., Arfanakis, K., Arvanitakis, Z., Leurgans, S.E., Turner, A.D., Barnes, L.L., Bennett, D.A., Buchman, A.S., 2015. Physical activity, motor function, and white matter hyperintensity burden in healthy older adults. Neurology. 84 (13), 1294–1300.
Vesperman, C.J., Pozorski, V., Dougherty, R.J., Law, L.L., Boots, E., Oh, J.M., Gallagher, C.L., Carlsson, C.M., Rowley, H.A., Ma, Y., Bendlin, B.B., Asthana, S., Sager, M.A., Hermann, B.P., Johnson, S.C., Cook, D.B., Okonkwo, O.C., 2018. Cardiorespiratory fitness attenuates age-associated aggregation of white matter hyperintensities in an at-risk cohort. Alzheimers Res Ther. 10 (1).
Palta P, Sharrett AR, Gabriel KP, et al. Prospective Analysis of Leisure-Time Physical Activity in Midlife and Beyond and Brain Damage on MRI in Older Adults. *Neurology*. 2021;96(7):e964-e974.
Tarumi, T., Tomoto, T., Repshas, J., Wang, C., Hynan, L.S., Cullum, C.M., Zhu, D.C., Zhang, R., 2021. Midlife aerobic exercise and brain structural integrity: Associations with age and cardiorespiratory fitness. Neuroimage. 225, 117512.
Wartolowska, K.A., Webb, A.J.S., 2021. Midlife blood pressure is associated with the severity of white matter hyperintensities: analysis of the UK Biobank cohort study. Eur Heart J. 42 (7), 750–757.
Garnier-Crussard A, Bougacha S, Wirth M, et al. White matter hyperintensities across the adult lifespan: relation to age, Aβ load, and cognition. *Alzheimers Res Ther*. 2020;12 (1):127.
Lampe, L., Zhang, R., Beyer, F., Huhn, S., Kharabian Masouleh, S., Preusser, S., Bazin, P.-L., Schroeter, M.L., Villringer, A., Witte, A.V., 2019. Visceral obesity relates to deep white matter hyperintensities via inflammation. Ann Neurol. 85 (2), 194–203.
Griffanti, L., Jenkinson, M., Suri, S., Zsoldos, E., Mahmood, A., Filippini, N., Sexton, C.E., Topiwala, A., Allan, C., Kivimäki, M., Singh-Manoux, A., Ebmeier, K.P., Mackay, C. E., Zamboni, G., 2018. Classification and characterization of periventricular and deep white matter hyperintensities on MRI: A study in older adults. Neuroimage. 170, 174–181.
Shen, X., Ma, S., Vemuri, P., Simon, G., 2020. Challenges and Opportunities with Causal Discovery Algorithms: Application to Alzheimer's Pathophysiology. Scientific Reports. 10 (1).